

TABLE I. Spatial geometry.

	Experiment			Theory (Ref. 1)		
	$r(\text{\AA})$	θ	ϕ	$r(\text{\AA})$	θ	ϕ
P_1	1.18	90°	0°	1.12	90°	0°
P_2	1.67	2.2°	180°	1.67	1.1°	180°
P_3	1.67	177.8°	180°	1.67	178.9°	180°
C_1	0.37	0°	0°	0.60	0°	0°
C_2	0.37	180°	0°	0.60	180°	0°

two carbon ions and three protons. The position and time of each fragment ion are converted on-line into a cluster ("molecule") velocity vector. This 15-dimensional velocity is reduced to nine "body" degrees of freedom.

To display the bridged proton structure we project the data in the following manner. For every molecule observed we choose the Z axis to be along the measured C-C velocity vector with the origin located symmetrically between the carbons. The X axis for each molecule is determined by the proton that is found to have the maximal velocity vector relative to the Z axis. The fragments are rotated about the C-C axis so that this chosen proton lies in the XZ plane with a positive X component. A contour plot of the density of all the ions projected onto the XZ plane is shown in Fig. 1. In the isometric plot above it one sees the two carbons in the center, the bridged proton (chosen to be on the XZ plane) and the other two groups of protons lying close to the C-C axis. The five particle groups can be separated easily to give an average velocity-space geometry (nine degrees of freedom) and a covariance matrix representing the full correlated deviations from the average geometry.

The average VS geometry thus determined is consistent with a planar molecule and a symmetry plane perpendicular to the C-C axis. A five-ion trajectory calculation code was

used to produce a geometrical structure from the average VS structure. For simplicity, pure Coulomb interactions were assumed. These preliminary structural parameters are compared with theoretical values for the nonclassical isomer in Table I. The small C-C distance we deduce in this way (0.74 Å) is a consequence of assuming the carbon fragment ions to be point charges. This underestimates the C-C force for such electron-rich ions at distances up to ~ 1 Å. The H-C forces are not as severely affected by this assumption. The resemblance of the experimental results to the calculation is striking, especially in view of the simplistic assumptions adopted in the analysis.

We have shown that it is possible to obtain average geometries directly. Beyond this, these data also contain the correlation of the fluctuations from this average. Further, detailed analysis of these data will yield more precise values for both the average geometry and the vibrational modes and frequencies.⁷

We wish to acknowledge several stimulating conversations with Professor R. S. Berry and thank him for pointing out the importance of this problem. This work is supported by the U. S. Department of Energy, Office of Basic Energy Sciences, under Contract No. W-31-109-ENG-38.

^{a)} Present address: Technion, Haifa, Israel 32000.

¹G. P. Raine and H. F. Schaefer, *J. Chem. Phys.* **81**, 4034 (1984); T. J. Lee and H. F. Schaefer (to be published).

²T. Oka (private communication).

³G. Both, E. P. Kanter, Z. Vager, and D. Zajfman, *Rev. Sci. Instrum.* (to be published).

⁴D. S. Gemmell, *Chem. Rev.* **80**, 301 (1980) and references therein.

⁵I. Plessner, Z. Vager, and R. Naaman, *Phys. Rev. Lett.* **56**, 1559 (1986).

⁶A. Faibis, W. Koenig, E. P. Kanter, and Z. Vager, *Nucl. Instrum. Methods B* **13**, 673 (1986).

⁷Z. Vager, E. P. Kanter, G. Both, P. J. Cooney, A. Faibis, W. Koenig, B. J. Zabransky, and D. Zajfman, *Phys. Rev. Lett.* (to be published).

Coherent photodissociation reactions: Observation by a novel picosecond polarization technique

J. S. Baskin, D. Semmes, and A. H. Zewail

Arthur Amos Noyes Laboratory of Chemical Physics,^{a)} California Institute of Technology, Pasadena, California 91125

(Received 23 September 1986; accepted 10 October 1986)

Photodissociation reactions have been studied by a variety of techniques that probe the initial (reagent) or final (product) state distribution(s) of the reaction.¹ With high-resolution lasers, one is able to obtain the population density^{1,2} of a given vibrational(v)-rotational(J) state. With picosecond/femtosecond lasers crossed with molecular beams, state-to-state rates are directly measured.³ An inter-

esting, and perhaps fundamental, question about the photodissociation process itself is this: Is molecular photodissociation a coherent process? In other words, if instead of exciting one vJ state one prepares a coherent superposition of vJ levels, would this superposition "survive" the dissociation process? Such coherence has not been detected before, perhaps because the laser coherence was not adequate or the pulses

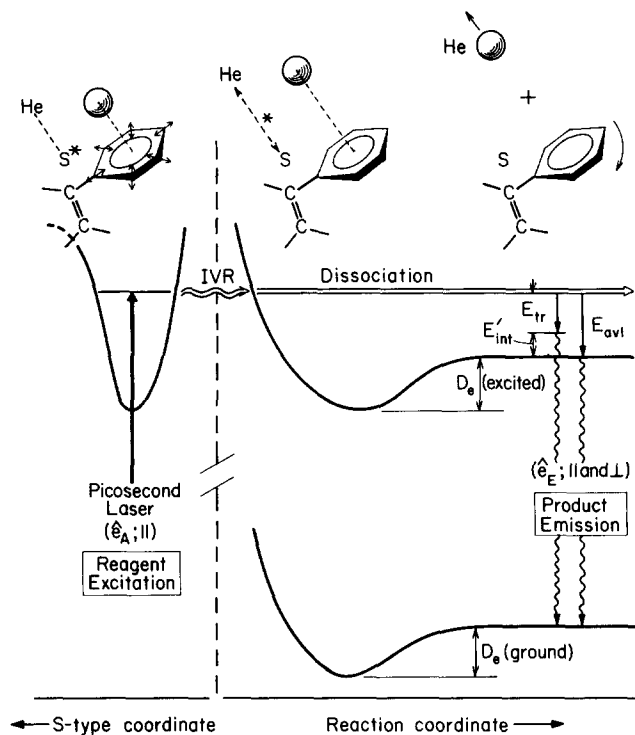


FIG. 1. Potential energy surface description of photodissociation and probing of coherence. \hat{e}_A and \hat{e}_E are the polarization vectors for vdW complex absorption and nascent product emission, respectively. D_e is the binding energy of the complex. The optically-excited stilbene-type mode of the complex is represented on the left-hand side of the figure. Energy reaches the reaction coordinate (right-hand side) via intramolecular vibrational energy redistribution (IVR). After dissociation (far right) the available energy is partitioned between translation (E_{tr}) and internal excitation of stilbene (E'_{int}).

used were not short enough in duration.

In this communication, we wish to report on a novel picosecond polarization method for measuring the degree of rotational coherence that is preserved in photodissociation reactions. The systems studied here are jet-cooled van der Waals molecules; stilbene⁴⁻⁶ bound⁵ to He or Ne with a 1:1 composition.⁷

Figure 1 gives the potential energy description of the experiment. A polarized picosecond laser-pulse coherently excites the νJ levels of a well-known stilbene-type mode⁴ (83, 95, or 198 cm^{-1}) in S_1 of the vdW complex. This creates an initial alignment. By IVR, energy transfers to the reaction coordinate, and the available energy partitions to translation and internal νJ excitation in nascent stilbene. The rising emission of nascent stilbene is then viewed with parallel and perpendicular polarizations (with respect to the initial pulse polarization). From these experiments, the IVR/photodissociation rates are measured from the decay of the complex and the buildup of the nascent, while the loss of coherence or alignment is determined from the observation of rotational recurrences.⁷

The picosecond/beam apparatus is described elsewhere.⁸ To this apparatus we added a polarizer/analyzer system so that the fluorescence can be analyzed prior to dispersion in the spectrometer.

Figure 2 gives the experimental results, frequency- and time-resolved at 83 cm^{-1} excitation. Similar studies were made for 95 and 198 cm^{-1} excitations, and for $S \cdot \text{Ne}$. When

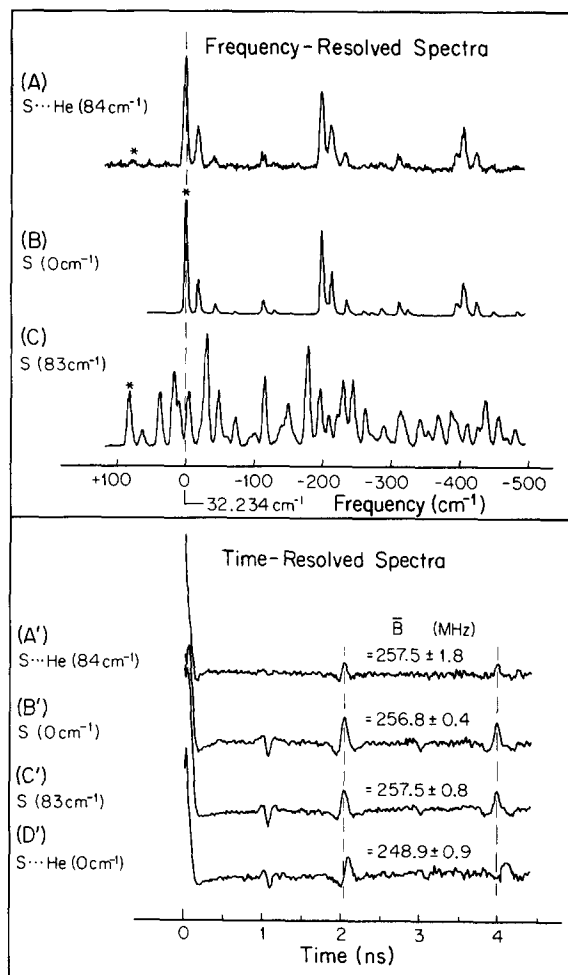


FIG. 2. Time- and frequency-resolved spectra of stilbene and stilbene-helium (1:1) complex. Excitation energies relative to the respective (complex or molecule) 0_0^0 transition energies are given at left. Excitation frequencies are marked by an asterisk in the upper spectra. Spectral resolutions for (A), (B), and (C) are 4, 1, and 5 cm^{-1} , respectively. The difference in resolution accounts for the broadening of (A) relative to (B). The time-resolved data is presented in the form of polarization anisotropies. Temporal resolution was about 60 ps FWHM for all measurements. \bar{B} is $\frac{1}{2}(B + C)$ of the complex or parent stilbene. Typical beam conditions are 500 psig for the complex, X/D ~ 60 , and temperature $\sim 150^\circ\text{C}$.

exciting $S \cdot \text{He}$ at 84 cm^{-1} we observe product(S) emission that entirely mimics the emission of parent S from 0 cm^{-1} (0° level) excitation (spectra A and B), consistent with previous observations.⁵ If parent stilbene is excited to 83 cm^{-1} , however, the emission is much different (C spectra) and exhibits resonant bands that have been analyzed in detail before.⁴ The available translational energy is therefore $> 30 \text{ cm}^{-1}$ since we know that the vdW bond energy is 50 cm^{-1} or less.

The time-resolved data are displayed here as anisotropies $r(t)$, i.e., picosecond decays with parallel polarization minus decays with perpendicular polarization. This allows us to monitor the coherence from recurrence amplitudes and establish the identity of products from recurrence spacings (which directly give the rotational constants of S and $S \cdot \text{He}$).⁷ Exciting the complex at 83 cm^{-1} we observe product stilbene recurrences as shown by the comparison made in the figure (A', B', C'). These recurrences give precisely the rotational constant of stilbene in the excited state (257.5 ± 1.8

MHz), and conclusively identify the stilbene product.⁹ Exciting the complex 0° level, on the other hand, (spectrum D') gives different recurrences characteristic of the S·He (1:1) complex (248.9 ± 0.9 MHz) with the He being on the phenyl ring.⁷

The above results lead to the following important conclusions. The recurrences do survive the dissociation process at all excitation energies studied in the S·He system; *the initial alignment (J coherent excitation) in the complex is preserved in the product.* In this case, we also observe very little ($< 4 \text{ cm}^{-1}$) rotational excitation in the product, as evidenced by the emission linewidth. For S·Ne, the recurrences have not been observed which indicates that the ensemble-averaged coherence is lost. The recoil velocity in the center-of-mass is $\sim 5 \times 10^4$ and $\sim 2 \times 10^4$ cm/s for He and Ne systems, respectively. The He leaves stilbene very rapidly and the impulsive force on the benzene ring is relatively small. For Ne, the force is larger and the available energy is channeled^{10,11} into more rotations [torque on the stilbene; more tumbling (J) than spinning (K)], as evidenced by the severe broadening ($\sim 40 \text{ cm}^{-1}$) observed in the emission spectra of produced stilbene.

Theoretical treatments¹² of coherence and mode specificity in these half-collision systems is now very important. The reported picosecond technique probes directly (in real time), these photofragmentation coherences and product state rates, and implications to recoil dynamics is evident.

We have benefited from detailed and enlightening discussions with Professor R. B. Bernstein.

^{a)} Contribution No. 7477. This work is supported by a grant from the National Science Foundation (DMR-8521191).

¹For a recent review see: S. Buelow, M. Noble, G. Radhakrishnan, H. Reisler, C. Wittig, and G. Hancock, *J. Phys. Chem.* **90**, 1015 (1986).

²H. W. Cruse, P. J. Dagdigan, and R. N. Zare, *Faraday Discuss. Chem. Soc.* **55**, 277 (1973).

³J. L. Knee, L. R. Khundkar, and A. H. Zewail, *J. Chem. Phys.* **82**, 4715 (1985); **83**, 1996 (1985); N. F. Scherer, J. L. Knee, D. D. Smith, and A. H. Zewail, *J. Phys. Chem.* **89**, 5141 (1985).

⁴J. A. Syage, W. R. Lambert, P. M. Felker, A. H. Zewail, and R. M. Hochstrasser, *Chem. Phys. Lett.* **88**, 266 (1982); J. A. Syage, P. M. Felker, and A. H. Zewail, *J. Chem. Phys.* **81**, 4685, 4706 (1984); P. M. Felker, W. R. Lambert, and A. H. Zewail, *ibid.* **82**, 3003 (1985); *J. Phys. Chem.* **89**, 5402 (1985).

⁵T. S. Zwier, E. Carrasquillo, and D. H. Levy, *J. Chem. Phys.* **78**, 5493 (1983); C. A. Taatjes, W. B. Bosma, and T. S. Zwier, *Chem. Phys. Lett.* **128**, 127 (1986).

⁶A. Amirav and J. Jortner, *Chem. Phys. Lett.* **95**, 295 (1983); T. J. Majors, U. Even, and J. Jortner, *J. Chem. Phys.* **81**, 2330 (1984).

⁷J. S. Baskin, P. M. Felker, and A. H. Zewail, *J. Chem. Phys.* **84**, 4708 (1986); P. M. Felker, J. S. Baskin, and A. H. Zewail, *J. Phys. Chem.* **90**, 724 (1986).

⁸W. R. Lambert, P. M. Felker, and A. H. Zewail, *J. Chem. Phys.* **81**, 2217 (1984); **82**, 2975 (1985).

⁹We have checked for the effect of collisions and bare stilbene absorption underlying the complex absorption. By careful distance and pressure dependence we determined that the complex absorption is definitely better than 95%.

¹⁰See, e.g., R. Bersohn, *J. Phys. Chem.* **88**, 5145 (1984); J. P. Simons, *ibid.* **88**, 1287 (1984).

¹¹K. W. Butz, D. L. Catlett, G. E. Ewing, D. Krajnovich, and Charles S. Parmenter, *J. Phys. Chem.* **90**, 3533 (1986); see also the excellent review by G. Ewing, *ibid.* **90**, 1790 (1986).

¹²For a recent review of work by the groups of Freed, Shapiro, Beswick, Jortner, and others, see: R. Schinke, *J. Phys. Chem.* **90**, 1742 (1986), and Ref. 11.

Coverage dependent phase transition of pyridine on Ag(110) observed by second harmonic generation

D. Heskett,^{a)} K. J. Song,^{a)} A. Burns,^{b)} E. W. Plummer,^{a)} and H. L. Dai^{b)}

Laboratory for Research on the Structure of Matter, University of Pennsylvania, Philadelphia, Pennsylvania 19104

(Received 26 September 1986; accepted 7 October 1986)

Due to symmetry conditions, second harmonic generation (SHG) from interfacial layers of a centrosymmetric metallic surface can be clearly identified.^{1,2} Such *surface* SHG has been recently applied to the study of well-characterized surfaces in ultrahigh vacuum. It has been shown that SSHG is sensitive to submonolayer adsorbate coverages³⁻⁵ and to surface structural changes.⁵ Although a microscopic understanding of the effects of adsorbates on SSHG is still required for this nonlinear optical phenomenon to be generally useful as a surface diagnostic tool, it is clear that certain surface processes can be identified through their influence on the SSHG. A coverage-dependent phase transition of pyridine on Ag(110) is reported here.

In the experiment of SHG from a Ag(110) surface, the 532 nm pulse from a Nd:YAG laser (Quanta-Ray DCR-

1A) was used as the fundamental light source. The surface was cleaned with ion bombardment and annealed to 400 °C in a chamber with $P < 10^{-10}$ Torr. The light was incident in the (001) plane of the crystal (the $x-z$ plane). The second harmonic intensity was detected without polarization analysis at specular angle by a photomultiplier tube after passing through a filter assembly. At a 45° laser incidence angle, SHG with both p - and s -polarization fundamental light were recorded [intensity hereafter denoted as $I_{2\omega}(p)$ and $I_{2\omega}(s)$] while the Ag(110) surface was exposed to oxygen, pyridine, and benzene.

$I_{2\omega}(p)$ was found to be 2.5 times larger than $I_{2\omega}(s)$ from the clean Ag(110) surface. This probably is due to the fact that because of the twofold surface symmetry in the dipole approximation of nonlinear susceptibility, χ_{zzz} , χ_{zxx} ,